

Electronic supplementary information (ESI) for

Preparation and characterization of tritycene-based microporous poly(benzimidazole) networks

Yan-Chao Zhao,^{a,b} Qian-Yi Cheng,^a Ding Zhou,^a Tao Wang,^a Bao-Hang
Han^{*,a}

^a *National Center for Nanoscience and Technology, Beijing 100190, China*

^b *Graduate University of Chinese Academy of Sciences, Beijing 100049,
China*

Tel: +86 10 8254 5576. Email: hanbh@nanoctr.cn.

Synthesis of 9,10-dimethyltriptycene-2,3,6,7,12,13-hexone

The monomer 9,10-dimethyl-2,3,6,7,12,13-hexahydroxytriptycene (100 mg) was suspended in ethanol (10.0 mL). To the suspension, a mixture of concentrated nitric acid (1.00 mL) and glacial acetic acid (1.00 mL) was added slowly while the temperature was kept at 0–5 °C. The mixture was stirred at room temperature for 24 h. The hexone product was then collected by filtration and washed with water and ethanol. After dried at 80 °C in a vacuum oven, a brown solid was obtained (56 % yield). M.p.: >300 °C; ^1H NMR (400 MHz, d^6 -DMSO): δ (ppm) 6.48 (s, 6H, Ar-*H*), 1.80 (s, 6H, -*CH*₃); IR (KBr, cm^{-1}): 3070, 2990, 1661, 1573, 1470, 1390, 1332, 1267, 1150, 1069, 894, 813, 683, 587.

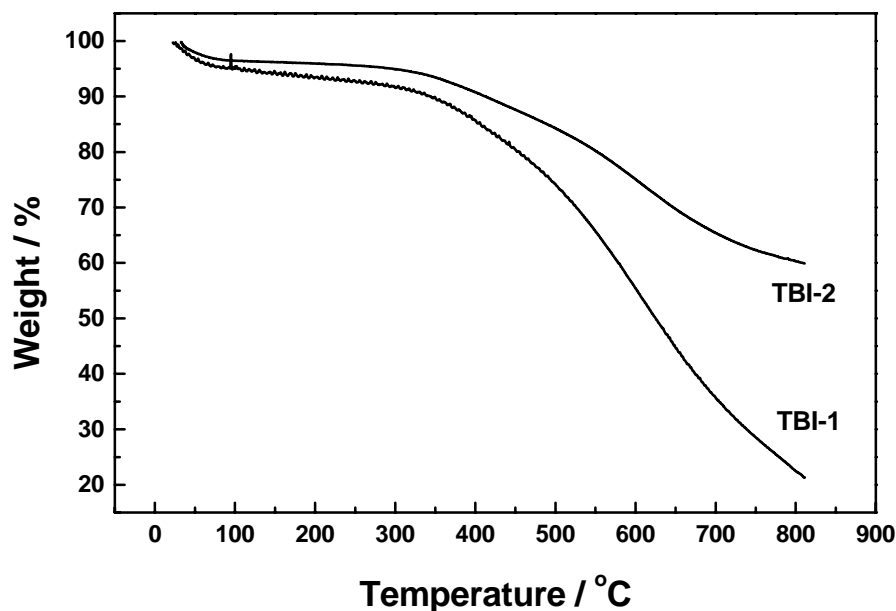


Figure S1. Thermogravimetric analysis (TGA) of **TBI-1** and **TBI-2**.

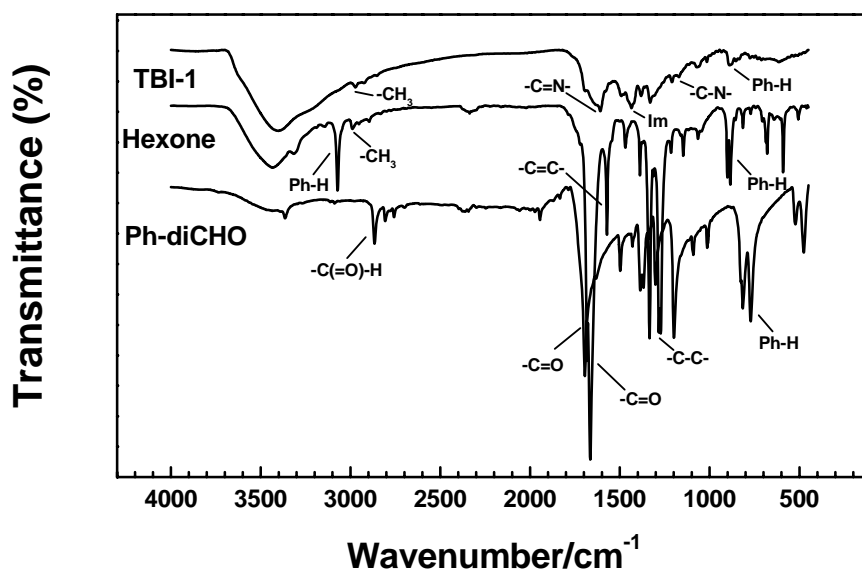


Figure S2. FT-IR spectra of hexone monomer, terephthalic aldehyde, and **TBI-1**.

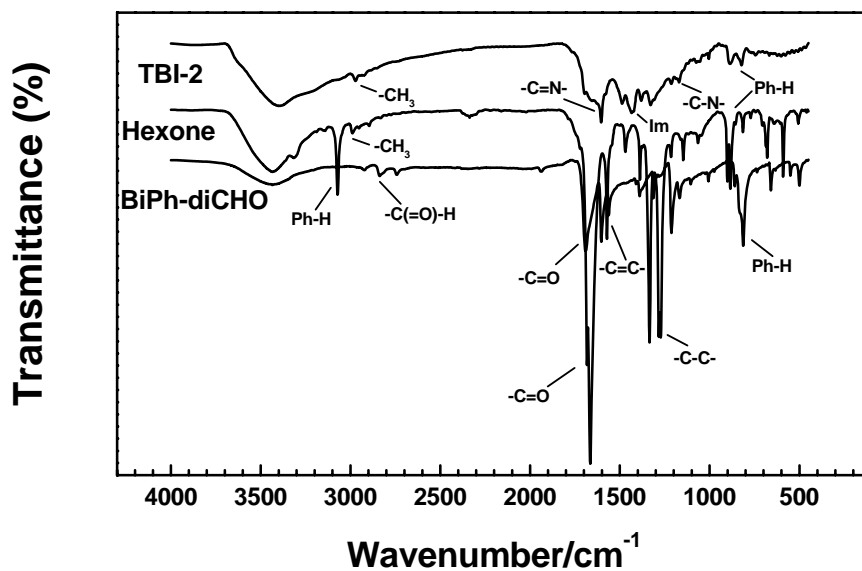


Figure S3. FT-IR spectra of hexone monomer, 4,4'-biphenyldicarboxaldehyde, and **TBI-2**.

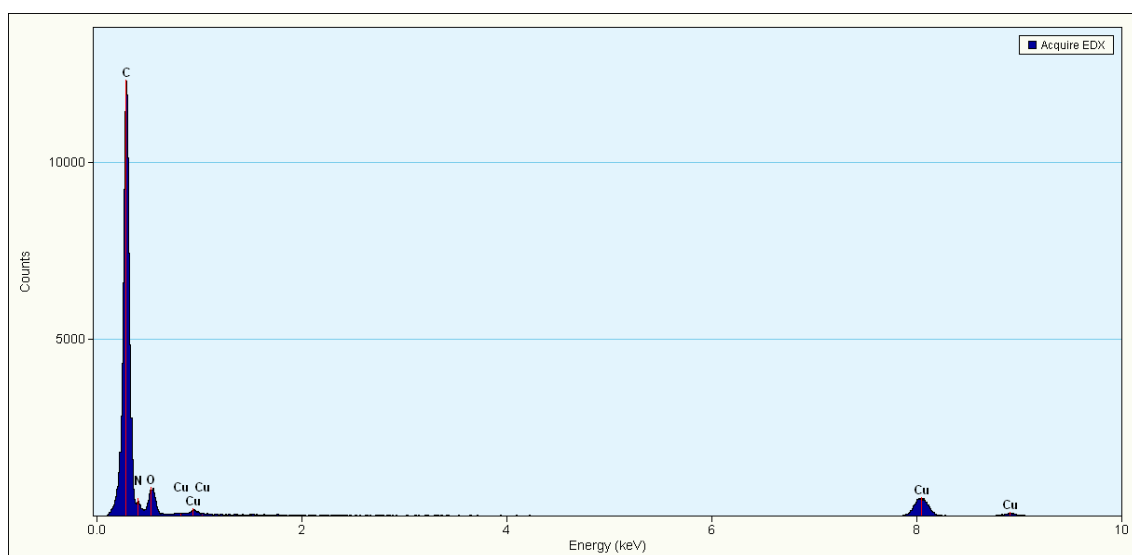


Figure S4. EDX spectrum for **TBI-1**.

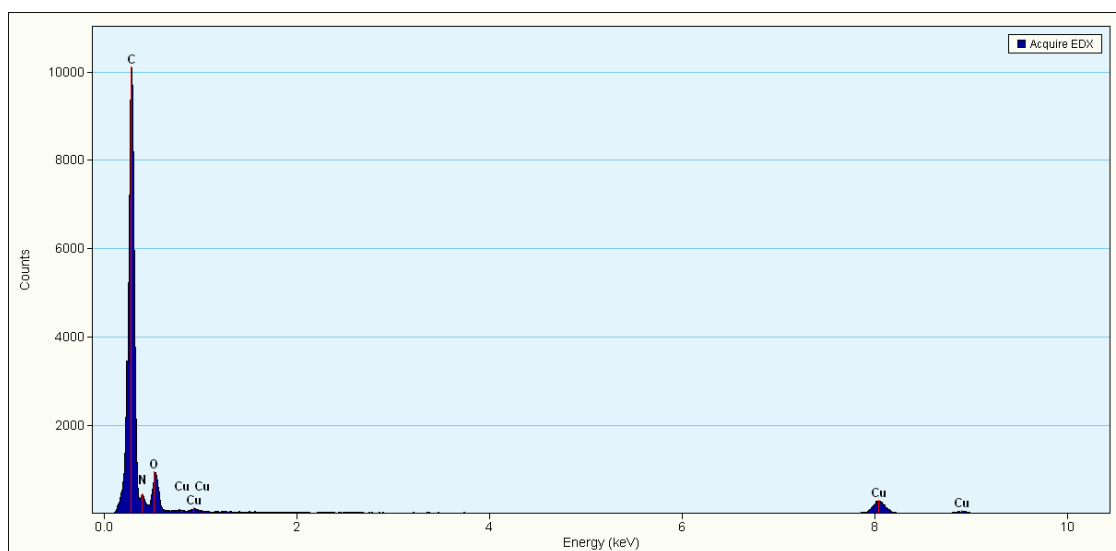


Figure S5. EDX spectrum for **TBI-2**.

Table S1. Elemental analysis for **TBI-1** and **TBI-2** (wt. %)

	Carbon	Hydrogen	Nitrogen
TBI-1 (Calcd.)	79.51	4.12	16.36
TBI-1 (Found)	69.94	4.24	15.28
TBI-2 (Calcd.)	81.88	4.79	13.32
TBI-2 (Found)	72.62	4.10	12.37

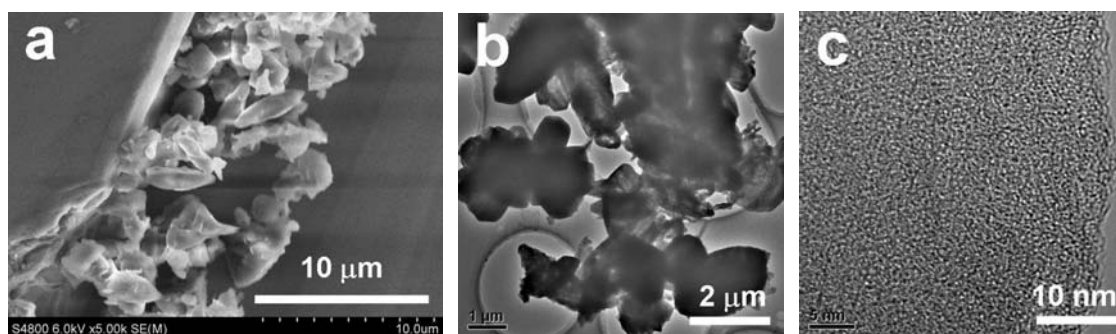


Figure S6. SEM (a), TEM (b), and HR-TEM (c) images of **TBI-1**.

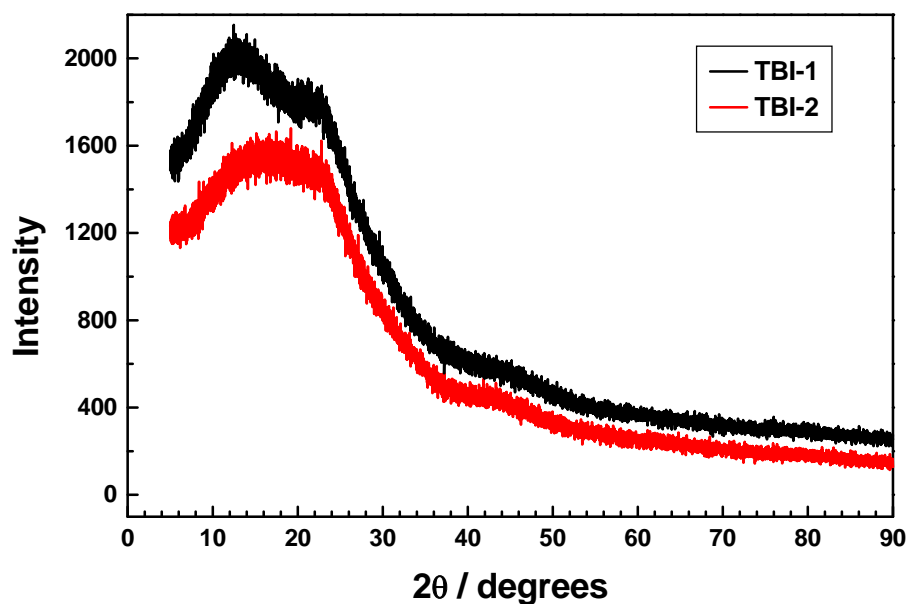


Figure S7. X-ray diffraction patterns of **TBI-1** and **TBI-2**.

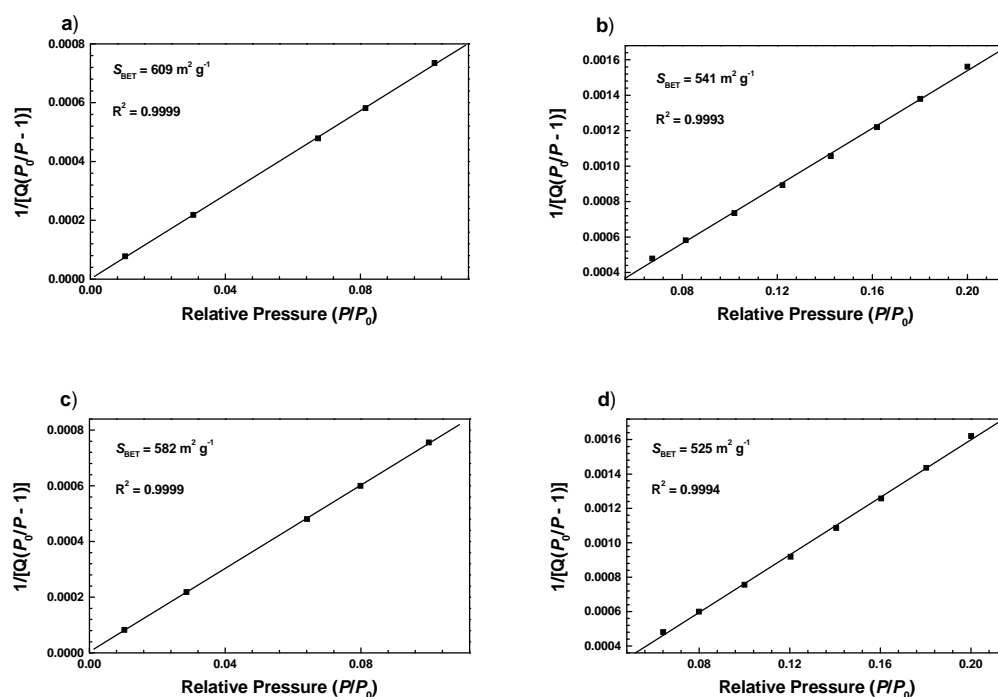


Figure S8. BET specific surface area plots for **TBI-1** (a, b) and **TBI-2** (c, d) calculated over different relative pressure ranges: $P/P_0 = 0.01-0.10$ (a, c) and $P/P_0 = 0.05-0.20$ (b, d), respectively.

Table S2. BET specific surface area data calculated over different pressure ranges

Sample	P/P_0 range	$S_{\text{BET}} (\text{m}^2 \text{ g}^{-1})$	Correlation coefficient	Points	C constant ^a
TBI-1	0.01–0.10	609	0.9999	5	12292
TBI-1	0.05–0.20	541	0.9993	8	-113
TBI-2	0.01–0.10	582	0.9998	5	1853
TBI-2	0.05–0.20	525	0.9994	8	-91

^a The low relative pressure range of 0.01–0.10 using five points gives the higher C constant values and therefore the best fit to the BET equation.

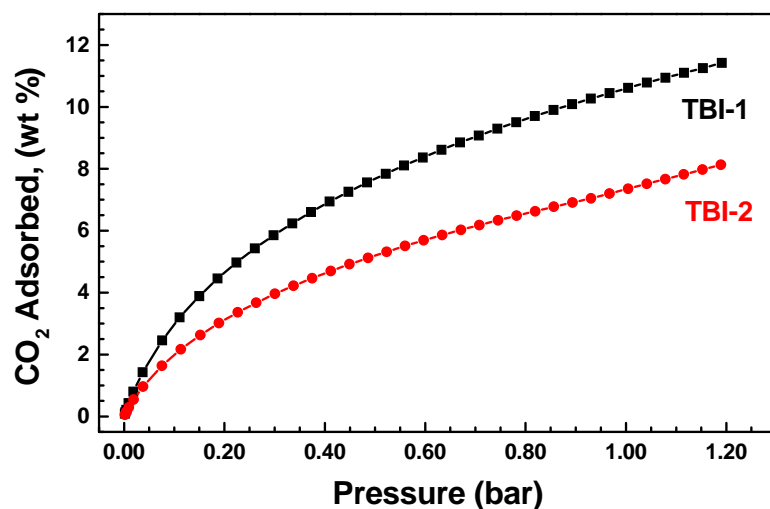


Figure S9. Carbon dioxide adsorption isotherms for **TBI-1** (black solid square) and **TBI-2** (red solid circle) at 288 K, respectively.

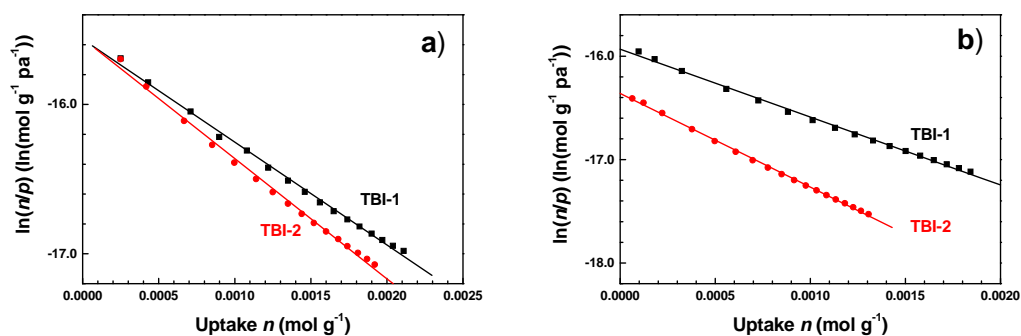


Figure S10. Virial analysis of the adsorption data for CO₂ on **TBI-1** (black solid square) and **TBI-2** (red solid circle) at 273 K (a) and 288 K (b) at low pressure range.

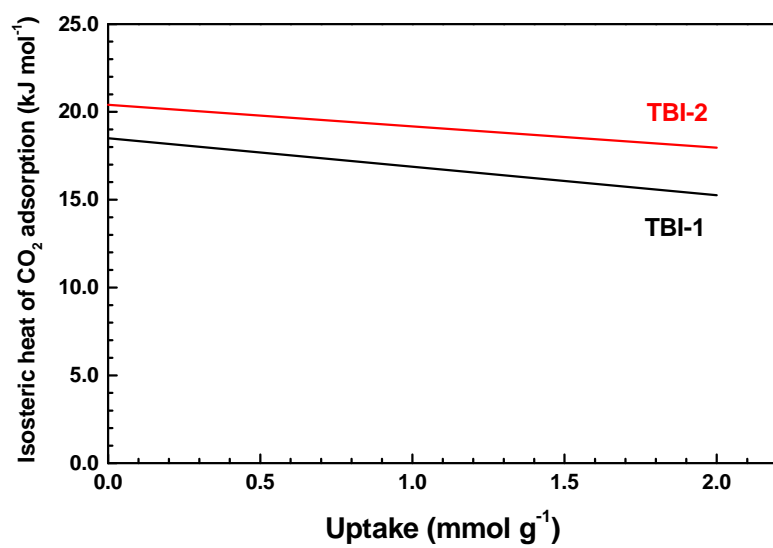


Figure S11. Variation of isosteric heat of adsorption with amount of adsorbed CO₂ in TBI-1 (black) and TBI-2 (red).